Dirac scatteredwave study of trigonal bipyramidal silver clusters Ag5 q+ (q=0, 2–4)

Ramiro ArratiaPerez and Gulzari L. Malli

Citation: The Journal of Chemical Physics **85**, 6610 (1986); doi: 10.1063/1.451443
View online: http://dx.doi.org/10.1063/1.451443
View Table of Contents: http://scitation.aip.org/content/aip/journal/jcp/85/11?ver=pdfcov
Published by the AIP Publishing

Dirac scattered-wave study of trigonal bipyramidal silver clusters Ag_5^{q+} ($q=0,2-4$)

Ramiro Arratia-Perez[a] and Gulzari L. Malli
Department of Chemistry and Theoretical Sciences Institute, Simon Fraser University, Burnaby, British Columbia, Canada V5A 1S6

(Received 22 April 1986; accepted 22 August 1986)

The electronic structure of the neutral and cationic pentaatomic silver bare clusters is investigated by the Dirac scattered-wave (DSW) method. The results indicate that there is significant $5s_{1/2}$–$4d_{5/2}$ hybridization in the bonding molecular orbitals, due to relativistic effects. Molecular hyperfine interactions (hfi) are calculated for the paramagnetic species Ag_5^{q+} ($q=0$, 2, and 4) through a *first-order perturbation* to the Dirac Hamiltonian. The ground state ($^2E'$) orbital degeneracy of Ag_5 in D_{3h} geometry is removed by spin-orbit interaction leading to Kramers degeneracy, and consequently the D_{3h} geometry of Ag_5 will not distort due to Jahn–Teller effect. It is found that the hyperfine coupling constants calculated by using a four-component wave function for the Ag_5^{2+} and Ag_5^{4+} clusters differ significantly from previously computed hfi using a *second-order perturbation* to the Schrödinger Hamiltonian. First ionization potentials and excitation energies are predicted for all the species as calculated by the spin-restricted transition state method.

I. INTRODUCTION

The study of bare silver clusters is of great interest in such areas as surface physics and chemistry, the photographic process, and heterogeneous catalysis.[1–3] A representative example includes ultrafine dispersed naked silver clusters formed via the controlled aggregation of metal atoms in low temperature matrices.[4–6] The UV and visible absorption spectra of the silver aggregates have been studied as a function of their size.[7–9] In addition, the ESR spectra of small silver clusters ($n\leqslant 8$) in several inert matrices have been reported,[5,6,10] and in particular, from the tentative assignment of the ESR spectra of Ag_5 in adamantane and cyclohexane, a trigonal bipyramidal (D_{3h}) geometry with Jahn–Teller distortion was proposed.[11,12]

Ab initio nonrelativistic LCAO-MO-SCF calculations have been carried out for a series of Cu_n clusters ($n=2$–5, 8, and 13),[13] and for the Cu_5 cluster the trigonal bipyramidal geometry is predicted to be of the lowest energy. Recently, the excitation energies and the first ionization potentials of trigonal bipyramidal Ag_5^{q+} ($q=0$–4), as well as, the g- and hyperfine (A) tensor components for Ag_5^{2+} and Ag_5^{4+} have been predicted by Ozin, Mattar, and McIntosh (OMM)[14] through a nonrelativistic SCF scattered-wave calculation.[15(a)] It will be interesting to compare these nonrelativistic calculations[14] based on a second-order perturbtion treatment in which the spin-orbit and nuclear hyperfine interaction were treated as perturbation to the Schrödinger Hamiltonian, with the present DSW calculations where we use a four-component wave function[15(b)] which includes the relativistic corrections (Darwin, mass-velocity, and spin-orbit) at the SCF stage. Molecular hyperfine interactions are then calculated by *first order perturbation* (the nuclear hyperfine interaction) to the Dirac Hamiltonian.[16] The above mentioned (OMM) and the present DSW approach solve the eigenvalue problem by using the multiple scattering technique,[15] and both these spin-restricted approaches neglect spin-polarization effects that can be important for the clusters studied here.

Hyperfine interactions in molecular radicals can be an important source of information about molecular electronic structure and chemical bonding characteristics. For most radicals the observed tensors can be decomposed into an isotropic Fermi term and a traceless spin-dipolar contribution. Radicals containing heavy atoms, however, are often complicated by orbital contributions to the hyperfine tensors arising from spin-orbit mixings with the excited states.[16] Because these contributions from electronic orbital motion are neither isotropic nor traceless, one cannot make a simple decomposition of the hyperfine tensors into isotropic and anisotropic parts.[16] There are some situations in which this procedure may be expected to break down; e.g., (a) when the unpaired spin is not localized on a single center as in the present case, where the unpaired electron is uniformly distributed amongst the various metal centers with appreciable spin-orbit constants; (b) the valence molecular energy levels are very close together so that a first order perturbation treatment of spin-orbit mixings is expected to be inadequate.

In this paper we present an alternative approach to the calculation of molecular hyperfine interactions in which we use relativistic (Dirac) wave functions as the starting point.[16] Since these wave functions include spin-orbit effects (and transform according to the molecular double point group), only the nuclear hyperfine interaction need be included in the perturbation scheme.[16] The results of this approach are compared with those of Ozin *et al.* (OMM)[14] who started from a nonrelativistic wave function and treated the spin-orbit operator and the nuclear hyperfine interaction as perturbations.

The organization of this paper is as follows. Section II outlines the calculational procedure, and in Sec. III we present our molecular orbital analysis, hyperfine interactions assignments, and transitions state results. In Sec. IV we summarize our conclusions.

[a] Current address: Department of Chemistry, University of Texas at Arlington, Box 19065, Arlington, Texas 76019.

 0021-9606/86/236610-13$02.10

II. METHOD OF CALCULATION

The self-consistent-field Dirac scattered-wave (SCF-DSW) molecular orbital method is the relativistic extension[15(b)] of the nonrelativistic scattered-wave technique originally developed by Johnson.[15(a)] The DSW methodology has been extensively reviewed[17–19] and was first developed by Yang and Rabii[15(b)] for calculations of bound-state wave functions. This method uses the same potential and exchange approximations as in the conventional nonrelativistic scattered-wave theory, but uses the Dirac equation rather than the Schrödinger equation to generate the one-electron orbitals. Thus, the relativistic effects such as spin-orbit interaction, Darwin, and mass-velocity corrections are included at the SCF stage. For each orbital, the wave function inside the atomic spheres is written as a linear combination of atomic spinors $|\kappa,\mu\rangle$ where

$$|\kappa,\mu\rangle = \begin{pmatrix} g(r)\chi_{\kappa\mu}(\theta,\phi) \\ if(r)\chi_{-\kappa\mu}(\theta,\phi) \end{pmatrix}. \tag{1}$$

In Eq. (1), the $g(r)$ and $f(r)$ are the radial functions determined by numerical integration of the radial Dirac equations and the $\chi_{\kappa\mu}(\theta,\phi)$ are the two-component spherical spinors.[20] The molecular potential is the sum of the Coulomb potential arising from the nuclei and electrons, and an exchange-correlation term, for which Slater's local density approximation[21] is used. The orbital energies are determined by solving the DSW secular equations and the resulting molecular spinors transform according to the extra irreducible representations (irrep) of the molecular double point group.

The method used for the calculations of the hyperfine interactions has been described elsewhere,[16,22] and is based upon a first order perturbation to the Dirac Hamiltonian so that the effects of magnetic fields are described by the perturbation operator[16] $\mathscr{H}$, where

$$\mathscr{H} = e\boldsymbol{\alpha}\cdot\mathbf{A}\,. \tag{2}$$

In Eq. (2) $\boldsymbol{\alpha}$ is the vector of 4×4 Dirac matrices and $\mathbf{A}$ is the electromagnetic vector potential. For the hyperfine term $\mathbf{A} = (\boldsymbol{\mu}\times\mathbf{r})/r^3$, where μ is the nuclear magnetic moment. Matrix elements of these operators are evaluated for the two rows of the twofold irreps of the molecular orbitals holding the unpaired electron. The details of the evaluation of the angular and the radial integrals have been described earlier.[16,22] The resulting perturbation energies are then fitted to the usual spin Hamiltonian for anisotropic hyperfine interactions,

$$\mathscr{H}\,\text{spin} = \sum_n \mathbf{S}\cdot\mathbf{A}_n\cdot\mathbf{I}_n\,, \tag{3}$$

where in Eq. (3), a value of $S = \frac{1}{2}$ is used to describe the ground state Kramers doublet, and I_n is the nuclear spin ($I = \frac{1}{2}$ for ^{109}Ag or ^{107}Ag), A_n is the hyperfine coupling constant, and n = Ag(axial) or Ag(equatorial). Since $\mathscr{H}$spin is evaluated over the electron spin functions in a basis for which S_z is diagonal, in order to compare the matrix elements, the molecular Dirac spinors are rotated so that the z component of $(r\times\alpha)/r^3$ is also diagonal. Hence, the matrix elements of $\mathscr{H}$ may be directly identified with those of $\mathscr{H}$spin,[16,22]

$$\begin{aligned} A_{ix} &= 2eg_N\beta_N\,\mathrm{Re}\langle 1|(\mathbf{r}\times\boldsymbol{\alpha})_i/r^3|2\rangle\,, \\ A_{iy} &= 2eg_N\beta_N\,\mathrm{Im}\langle 1|(\mathbf{r}\times\boldsymbol{\alpha})_i/r^3|2\rangle\,, \quad i = x,y,z \\ A_{iz} &= 2eg_N\beta_N\langle 1|(\mathbf{r}\times\boldsymbol{\alpha})_i/r^3|1\rangle\,, \end{aligned} \tag{4}$$

In Eq. (4) A_{ii} are the hyperfine tensor components as defined in Eq. (3), g_N is the nuclear g factor, β_N is the nuclear magneton, and 1 and 2 label the rows 1 and 2, respectively, of the highest occupied orbital.

This approach has been shown to be successful in calculating magnetic resonance parameters for heavy diatomic radicals,[16] transition metal,[23] lanthanide,[22] and actinide[24] complexes, as well as, in low nuclearity gold and silver clusters.[25] Here we report the application of this theoretical approach to calculate molecular hyperfine interactions in ligand-free pentaatomic silver trigonal bipyramidal clusters Ag_5^{q+} ($q = 0$, 2, and 4).

The various parameters used in these calculations are the same as those of Ozin *et al.* (OMM),[14] and the coordinate system for the M_5 cluster under D_{3h} symmetry is illustrated in Fig. 1. The partial wave expansions for the metal and the outer sphere were truncated at $l = 2$ and $l = 4$, respectively. The symmetrized basis functions of the double group D_{3h}^{*} were generated according to the procedure developed by Yang,[26] and our notation for the two-dimensional extra irreps is related to the Bethe's notation as follows: $e_1\leftrightarrow\gamma_7$, $e_2\leftrightarrow\gamma_8$, and $e_3\leftrightarrow\gamma_9$. The relationships between the single (D_{3h}) and the double (D_{3h}^{*}) group irreps indicate that the nonrelativistic (NR) doubly degenerate e' and e'' representations split into $e_2 + e_3$ and $e_1 + e_3$ extra irreps, respectively.[27] Furthermore, the nondegenerate pairs (a_1'' and a_2'') and (a_1' and a_2') of single group representations correlate with the two-dimensional e_2 and e_1 extra irreps, respectively, of the double group D_{3h}^{*}. The nonrelativistic limit (NR) results were obtained by using a large value of $c = 10^{15}$ a.u. in order to estimate quantitatively the relativistic effects. Each iteration of the SCF calculation required about 15 s on a CRAY-1 computer,[28] and about 40 iterations were required to achieve convergence.

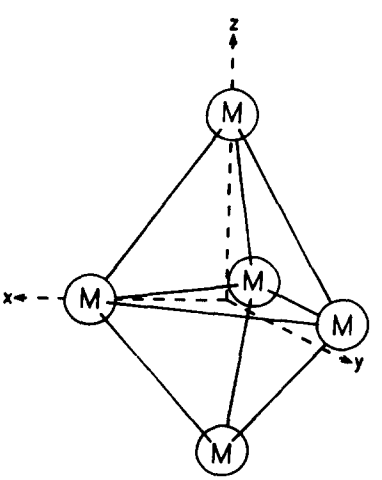

FIG. 1. The M_5 cluster.

III. RESULTS AND DISCUSSION

A. Molecular orbitals

The calculated relativistic (DSW) and the nonrelativistic (NR) orbital energies for Ag_5 are shown in Fig. 2. Here we also show the amount of 5*s* character mixed into the valence molecular orbitals. The NR results show a valence electronic structure which consists of a filled *d* band, partially filled *s*–*p* band, and an empty *p* band. The NR bonding characteristics of this silver neutral cluster were previously analyzed by OMM[14] and these are identical to our NR limit results. Both the SW-NR calculations predict the participation of the 4*d* metal orbitals in the cluster bonding scheme. A detailed analysis of the NR-MO's shows that the strongly bonding $4a_1'$ orbital consists mostly of 5*s* atomic combinations (~73%), whereas the other bonding MO's ($1a_1'$, $1a_2''$, $1e'$, $1e''$, and $2e'$) consist of almost pure 4*d* atomic combinations of the appropriate symmetry. The filled *d* band contains several antibonding MO's ($1a_1''$, $2a_2''$, $4e''$, $5e'$, and $3e''$), while the remaining MO's are essentially nonbonding combinations of the 4*d* silver orbitals. The filled $3a_2''$ and the partially occupied $6e'$ (HOMO) are mostly antibonding 5*s*–5*p* (66% 5*s* and 30% 5*p*) hybrid MO's. It should be noted from Fig. 2 that the valence molecular orbitals which constitute the occupied *d* band are very close together. This suggests that a first order perturbation treatment of spin-orbit mixings is expected to be inadequate. We shall return to this point later, where we will discuss the evaluation of the magnetic hyperfine interactions carried out by OMM[14] using nonrelativistic wave functions and the spin-orbit operator as a perturbation.

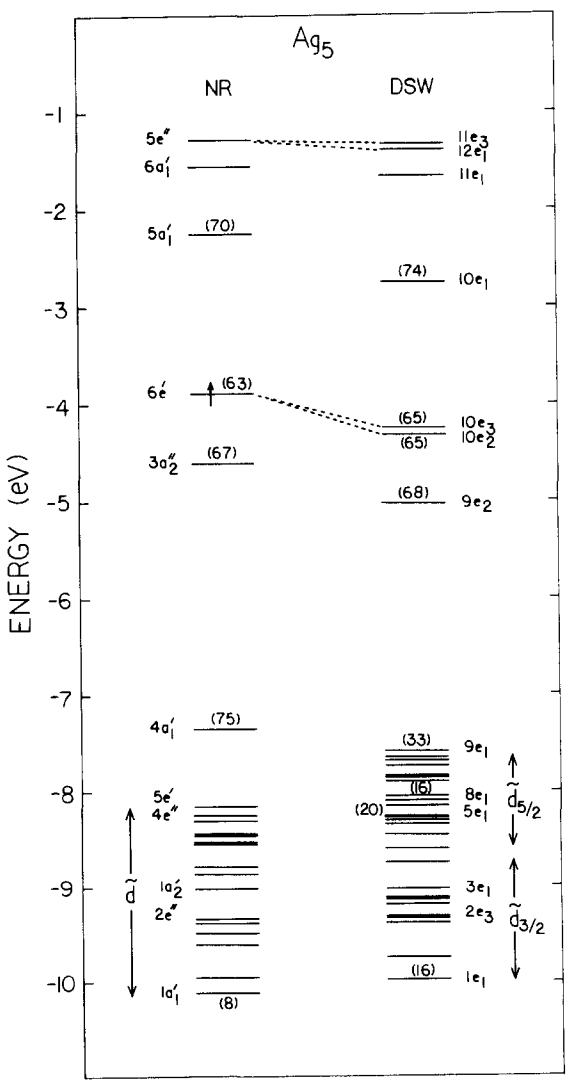

FIG. 2. Nonrelativistic (NR) limit and relativistic (DSW) valence energy levels of Ag_5. Numbers in parentheses give the percent 5*s* metal character, values less than 8% are not marked. The HOMO's are $6e'$ (NR) and $10e_2$ (DSW).

The valence electronic structure of Ag_5 as calculated by the relativistic (DSW) approach is illustrated in Fig. 2. Upon inclusion of relativity the occupied *d* band splits by spin-orbit interaction into the $d_{3/2}$ and the $d_{5/2}$ subbands by ~1.2 eV. The splitting of the valence *d* band has been observed in photoemission experiments on a low coverage of silver on a carbon substrate,[29] and in the photoelectron spectra of clean surfaces of Ag.[30] The DSW calculated values for the *d* band splitting on the trimeric and tetrameric silver clusters[25] are ~0.8 and ~0.9 eV, respectively. It is apparent that the *d* band splitting increases with the cluster size and the same trend has been observed experimentally.[29] In addition, relativistic effects in Ag_5 increase the *d* bandwidth by ~0.5 eV, as can be seen from Fig. 2. Since it is well known that relativistic effects stabilize the *s* and *p* orbitals, and destabilize the *d* orbitals in Ag atom,[31] the unoccupied ($10e_1$) and $10e_3$ (LUMO), and the occupied $10e_2$ (HOMO), $9e_2$ and $9e_1$ levels are stabilized in the Ag_5 cluster, while the occupied molecular orbitals lying in the *d* band are destabilized. These relativistic shifts of the molecular energy levels can also be appreciated from the total valence populations for Ag_5 given in Table I. Within the *d* populations the $d_{3/2}$ and $d_{5/2}$ spinors are equally populated, and the population ratio ($l+\frac{1}{2}$ to $l-\frac{1}{2}$) is 1.50 which is equal to the NR limit. However, among the *p* orbitals the lower energy $p_{1/2}$ spinors are favored over the $p_{3/2}$ spinors. The population ratios are 1.22 (axial) and 1.47 (equatorial) in the DSW calculation, but a value of 2.00 is required by symmetry in the NR limit. It becomes apparent that relativistic effects in this cluster are not very large, but they cannot be neglected.

Due to the relativistic stabilization of the 5*s*–5*p* hybrid molecular orbitals and the relativistic destabilization of the MO's located in the *d* band, significant "*s*–*d*" hybridization arises in the molecular orbitals ($9e_1$, $8e_1$, and $5e_1$) located in the $d_{5/2}$ band (see Fig. 2). This is a relativistic effect since it is not present in the NR description and it seems to be size dependent because in the DSW calculations on Ag_3^{2+} it was shown that the *s*–$d_{5/2}$ hybridization was negligible.[25] The degeneracy of the $6e'$ (NR-HOMO) is removed by spin-orbit interaction which splits it into the $10e_3$ (LUMO) and the $10e_2$ (HOMO) by ~600 cm^{-1} due to the $5p_{1/2}-5p_{3/2}$ contents.

The detailed analysis of the valence molecular orbitals indicates that the cluster bonding is dominated by the MO's of e_1 symmetry ($1e_1$, $5e_1$, and $9e_1$) that are significantly *s*–*d* hybridized. In Fig. 3 we show only the contours of the dominant component (in the *xy* plane) of the $9e_1$ (which is identical to the orbital shown in Ref. 14) and $5e_1$ bonding MO's. The contours of the $9e_1$ orbital in the *xz* plane show an *s*–*d*

TABLE I. Total valence populations for silver clusters.[a]

l	j	Ag_5	Ag_5^{2+}	Ag_5^{3+}	Ag_5^{4+}
s	$\frac{1}{2}$	1.030	0.648	0.312	0.199
	$\frac{1}{2}$	0.096	0.053	0.052	0.042
p		1.22[b]	1.79	1.77	1.71
	$\frac{3}{2}$	0.117	0.095	0.092	0.072
Total p		0.213	0.148	0.144	0.114
	$\frac{3}{2}$	3.946	3.949	3.948	3.937
d		1.50	1.49	1.50	1.49
	$\frac{5}{2}$	5.928	5.922	5.939	5.872
Total d		9.874	9.871	9.887	9.809
Total Ag (ax)		11.117	10.667	10.343	10.122
s	$\frac{1}{2}$	0.717	0.493	0.472	0.316
	$\frac{1}{2}$	0.155	0.092	0.062	0.054
p		1.47	1.72	1.71	1.62
	$\frac{3}{2}$	0.228	0.158	0.106	0.088
Total p		0.383	0.250	0.158	0.142
	$\frac{3}{2}$	3.924	3.924	3.916	3.920
d		1.50	1.50	1.50	1.49
	$\frac{5}{2}$	5.898	5.888	5.882	5.874
Total d		9.822	9.812	9.798	9.794
Total Ag(eq)		10.922	10.555	10.438	10.252

[a] The charge in the intersphere and outer sphere regions has been partitioned among the atoms, see Ref. 32.
[b] Ratio of population for the $j = l + \frac{1}{2}$ and $j = l - \frac{1}{2}$. For the nonrelativistic orbitals (not shown) these are required by symmetry to have the values $(l+1)/l$.

hybridized bonding MO which is illustrated in Fig. 4. This orbital should be contrasted with the $4a_1'$ bonding orbital shown by OMM[14] in Fig. 3(a), which is composed primarily of 5s atomic orbitals. It is interesting to note in Fig. 3, that the $5e_1$ wave function contours (xy plane) show a bonding molecular orbital. This is due to a relativistic effect (d orbital expansion) since the corresponding NR-MO ($3a_1'$) is nonbonding [see Fig. 5(b) of Ref. 14]. In addition, there are small bonding contributions from the molecular orbitals ($1e_2$, $1e_3$, $2e_2$, $2e_3$, $2e_1$, and $3e_2$) that are almost pure $4d_{3/2}$ combinations with small $4d_{5/2}$ admixtures. Furthermore, there are antibonding MO's which are either 5s–5p hybrids ($9e_2$ and $10e_2$) or mostly $4d_{5/2}$-like with small $4d_{3/2}$ admixtures ($6e_1$, $7e_1$, $7e_2$, $8e_3$, $8e_2$, and $9e_3$). The remaining MO's are mostly nonbonding.

As charge is depleted from the HOMO ($10e_2$) it is seen from Fig. 5, where we show the relativistic energy levels of the Ag_5^{q+} ($q = 2$–4) species, that the cluster bonding is mostly dominated by the molecular orbitals $1e_1$ and $9e_1$ that are s–d hybridized. The orbital $9e_1$ is illustrated for Ag_5^{3+} in Fig. 6. In Table I we present the total valence populations of the charged silver clusters. It can be seen, that as charge is depleted from the neutral cluster, the valence $5s_{1/2}$ and the total 5p populations decrease steadily and these contributions are concentrated in the $9e_1$ molecular orbital (see Fig. 5). It can also be appreciated from Table II that the $4d_{5/2}$

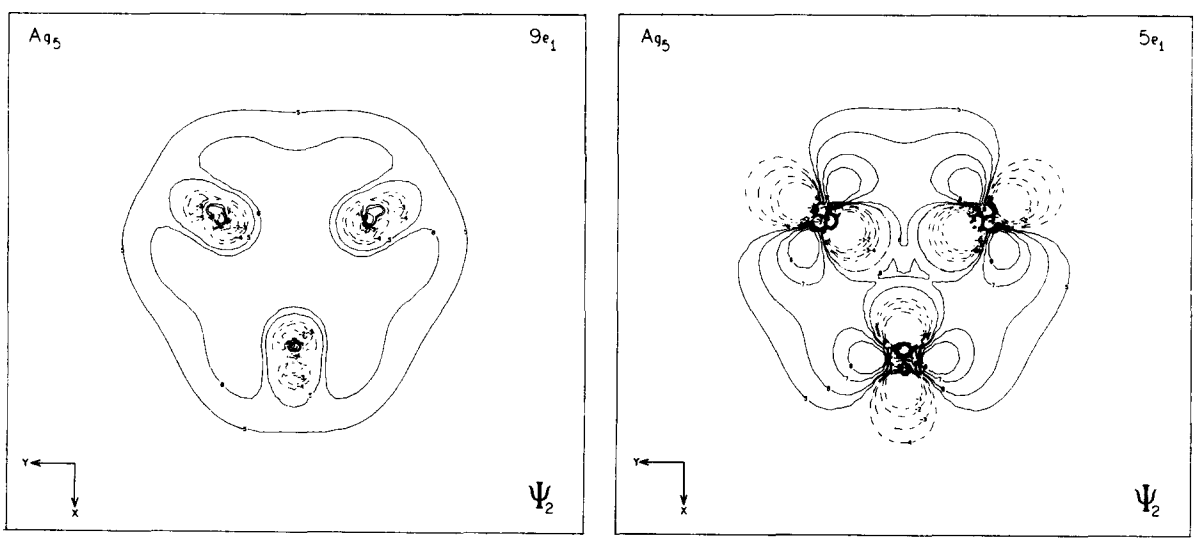

FIG. 3. Contours of the dominant $9e_1$ and $5e_1$ components (XY plane) of Ag_5. Contour values (in electron/bohr^3)$^{1/2}$ are between ± 0.06 and ± 0.01, and are the same for all the contours presented here. Negative wave function contours are given by dashed line.

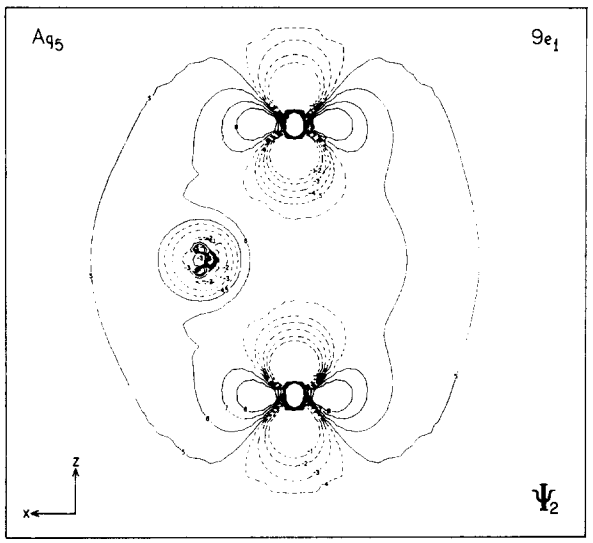

FIG. 4. Dominant component of $9e_1$ (XZ plane) of Ag_5.

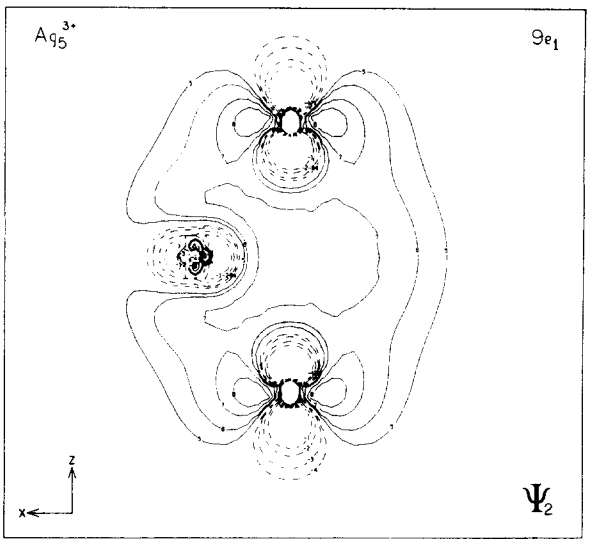

FIG. 6. Dominant component of $9e_1$ (XZ plane) of Ag_5^{3+}.

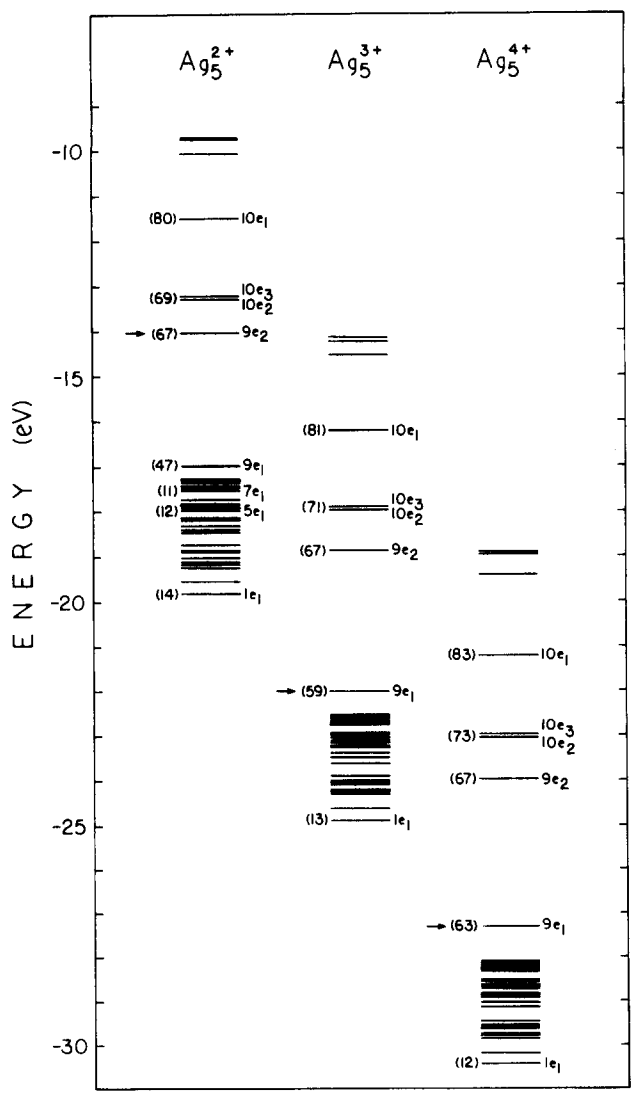

FIG. 5. Relativistic ground state valence energy levels of silver cationic clusters. The HOMO is indicated by an arrow in each case.

populations also decrease, in contrast to the statement that the 4*d* orbitals remain untouched upon this successive ionization process.[14]

It can be concluded that despite the qualitative usefulness of nonrelativistic calculations such as those described by Ozin *et al.*,[14] relativisitic effects remain crucial to describe correctly the valence electronic structure of heavy atom systems, and one should take into account the relativistic effects in order to obtain realistic bonding information in these trigonal bipyramidal silver clusters.

B. Spin distributions and hyperfine interactions

1. Ag_5

The neutral silver cluster Ag_5 has been prepared in cyclohexane and adamantane matrices and its ESR spectrum has been reported.[11,12] The favored geometry is trigonal bipyramidal D_{3h} (with a $^2E'$ ground state), which is postulated to be Jahn–Teller (dynamic) distorted by opening up the equilateral triangle, resulting in a $^2B_2$ (C_{2v}) ground state.[11,12] In such a case, the ESR spectrum was interpreted as that of an $S=\frac{1}{2}$ molecule containing two equivalent (equatorial) Ag atoms with large hyperfine interactions and three Ag atoms (two equivalent axial and one unique equatorial) with small hyperfine interactions.[11,12] It should be noted, however, that the experimental ESR parameters were calculated from solutions of an *isotropic* spin Hamiltonian (using the $M_I = \pm 1$ components), while the spectrum appears to be *anisotropic*. Here we report the calculated spin distributions and hyperfine coupling constants of Ag_5, assuming the D_{3h} geometry (as shown in Fig. 1), by using SCF-DSW four-component (Dirac) wave functions.

As we mentioned earlier, the nonrelativistic (NR) calculations on Ag_5 predict that the unpaired electron resides in an orbitally degenerate MO ($6e'$) with $^2E'$ ground state. Howard *et al.*[11,12] from the expected similarities between Cu_5 and Ag_5, and their INDO calculations[34] on Cu_5, stated that due to orbitally degenerate ground state the ESR spectrum *would not be visible*.[12] In order to explain the observed ESR spectrum they invoked the dynamic Jahn–Teller effect which would remove the orbital degeneracy. However, un-

TABLE II. Spin populations of Ag_5.

	Dirac[a]			Pauli[b]			
	l	j	Population	l	m	Spin	Population
D_{3h}							
	s	$\frac{1}{2}$	0.002	s	0	α	0.002
	p	$\frac{1}{2}$	0.080	p	1	β	0.012
Ax(2)	p	$\frac{3}{2}$	0.041	d	0	α	0.002
	d	$\frac{3}{2}$	0.020	d	1	β	0.038
	d	$\frac{5}{2}$	0.022	d	-2	β	0.030
	s	$\frac{1}{2}$	0.645	s	0	β	0.645
	p	$\frac{1}{2}$	0.093	p	0	α	0.001
Eq(3)	p	$\frac{3}{2}$	0.063	p	1	β	0.151
	d	$\frac{3}{2}$	0.016	p	-1	β	0.004
	d	$\frac{5}{2}$	0.018	d	1	α	0.001
				d	2	β	0.027
				d	-2	β	0.006
C_{2v}							
			Eq(2)[a]	Ax(2)			Eq(1)
	s	$\frac{1}{2}$	0.766	0.004			0.001
	p	$\frac{1}{2}$	0.004	0.024			0.023
	p	$\frac{3}{2}$	0.010	0.042			0.054
	d	$\frac{3}{2}$	0.002	0.014			0.009
	d	$\frac{5}{2}$	0.004	0.024			0.019

[a] In terms of atomic spinors.
[b] In terms of nonrelativistic functions, see the text.

der the relativistic (DSW) formalism, which uses double group theory throughout, the orbital degeneracy is removed by spin-orbit interaction which splits the NR-HOMO ($6e'$) into the twofold $10e_2$ and $10e_3$ MO's by $\sim 600\,cm^{-1}$, leading to a spin degeneracy (Kramers) into the HOMO ($10e_2$). Since, there is no orbital degeneracy in the ground state, the Jahn–Teller effect is not expected to be operative, and in addition, the twofold spin degeneracy cannot produce any instability of the molecular configuration[35] and thus would not distort the D_{3h} geometry in this cluster. Besides, the ESR spectra at 77 and 240 K showed essentially the same features, indicating thereby that there is no fluxional behavior of the Ag_5 cluster for this temperature range.[36] We also performed DSW calculations for this cluster under C_{2v} symmetry, by opening up the equilateral triangle to 84° (which was obtained from the pseudopotential CI and ECP calculations on Cu_3, see Ref. 33) and keeping the metal–metal distances (2.88 Å) unchanged.

The two rows of the HOMO ($10e_2$) correspond to the two components of the Kramers doublet and in the present spin-restricted calculations, all the spin density arises from the top occupied orbital. In Table II we present the spin populations of Ag_5. Here the charge in the intersphere and outersphere regions has been partitioned among the atoms according to the algorithm of Case and Karplus.[32] Two types of charge breakdown are shown. In the first, the charge is given in terms of the relativistic (Dirac) spinors; these are obtained directly from the coefficients of the solution to the DSW secular equations. The second breakdown uses a "nonrelativistic decomposition" in which only the two large components (Pauli) of the wave function are considered. In this procedure we assumed that the radial wave function inside each atomic sphere is the same for $l=j-\frac{1}{2}$ and $l=j+\frac{1}{2}$. The sum of two such spinors can then be interpreted as a nonrelativistic function of mixed spin; with spin α corresponding to column 1 and spin β to column 2. As shown in Table II, most of the unpaired electron is equally distributed on the equatorial silver atoms and is mainly of $5s$ (β) character (64.5%). The empirical estimates[11,12] suggest a value of $\sim 60\%$ ($5s$) and 20%–30% ($4d$ or $5p$) spin populations for the equatorial Ag nuclei. Our results show 15.6% contribution from $5p_{1/2}$, and $5p_{3/2}$, and 3.4% from ($4d_{3/2}$, $4d_{5/2}$). The remaining axial Ag nuclei have small $5s_{1/2}$ and $4d_{3/2}-4d_{5/2}$ spin populations and about 12% arises from $5p$ ($5p_{1/2}$, $5p_{3/2}$). Results of Pauli decomposition are also shown in Table II. In the NR limit (not shown) pure spin states are obtained, and one measure of the extent of spin-orbit mixings is the amount of minority spin mixed into the relativistic orbital. In this orbital ($10e_2$) the minority spin (α) is only 0.6% of the majority spin (β), and this will be reflected in small orbital contributions to the hyperfine tensors. However, it is interesting to note (Table II) that the axial set of Ag nuclei show a small (0.2%) $5s_{1/2}$ contribution that arises from spin-orbit contamination that will contribute a small Fermi term. In the NR limit this contribution is not allowed and hence the Fermi term will vanish by symmetry. In relativistic theory, the charge distribution for a $j=\frac{1}{2}$ state (either $s_{1/2}$ or $p_{1/2}$) is spherically symmetric, and its

contribution to the hyperfine tensors is isotropic, and in the neutral Ag_5 cluster most of the charge distribution (82%) arises from the $j = \frac{1}{2}$ states (see Table II). The contributions from the $j = \frac{3}{2}$ or $j = \frac{5}{2}$ states will result in anisotropic character to the hyperfine tensors. As shown in Table II these nonspherical contributions are not negligible (10% and 8% in Ag equatorial and Ag axial, respectively). In Table II we also present the calculated spin populations for Ag_5 in C_{2v} geometry, and it can be seen that most of the charge distribution arises from the two equivalent Ag (equatorial) nuclei and is mostly $5s$ (77%), while the remainder which consists mostly of $5p$ (16%) arises from the unique equatorial and the axial Ag nuclei. These populations are much larger than those estimated experimentally as well as those calculated for Ag_5 in the D_{3h} geometry. This would suggest that the calculated hyperfine coupling constants for the C_{2v} geometry will be much larger, and this is borne out by our calculations, as discussed below.

Results of the calculation of hyperfine coupling constants for Ag_5 are given in Table III, where we report the DSW values for both the D_{3h} and C_{2v} geometries. We have made an approximate decomposition of the relativistic (DSW) results into Fermi, spin dipolar ($A_{\rm dip}$), and orbital contributions (l_{ii}) as before.[16,22–25] A "Fermi" term can be defined as the diagonal contribution from the $s_{1/2}$ waves (which reduces to the conventional Fermi term in the NR limit). In a similar manner, we can define a "spin dipolar" contribution as the expectation value of $(3x^2 - r^2)/r^5$ evaluated over the relativistic wave function. This identification is only qualitatively useful, since the forms of the relativistic and nonrelativistic wave functions are different. Nevertheless, this decomposition allows us to identify some interesting features of relativistic effects on hyperfine interactions. In particular, by subtracting the Fermi and $A_{\rm dip}$ terms from the calculated total hyperfine interaction (A_{ii}), we can determine an "orbital contribution" (l_{ii}), an important quantity which is difficult to estimate by other methods.[16,22–24]

In Table III we show our calculated (DSW) and the experimental[11,12] values for the hyperfine coupling constants of Ag_5. It should be remarked that the experimental results were obtained for a Ag_5 cluster in solid matrices while our calculations should be applicable to the cluster in the gas phase. However, our calculations do not take into account the cluster–matrix interactions, which can exert a decisive influence in the geometry and structure of the entrapped metal cluster. Despite the above mentioned limitation, it would be informative to compare our results with those reported experimentally. It can be seen from Table III, that the hyperfine tensors are slightly *anisotropic* and arise mainly from the equatorial Ag nuclei. The calculated (for D_{3h} geometry) and the empirical estimate of the Fermi term are in good agreement, and both assignments agree that this is the major contribution to the observed hyperfine tensors. Furthermore, the experimental and the DSW (in D_{3h}) estimates of the $A_{\rm dip}$ contribution are a small portion of the total A_{ii}. However, our calculated values for the orbital terms are slightly larger than $A_{\rm dip}$, this is probably due to the contribution of the "small" components of the wave function. The small value of the orbital terms for the equatorial Ag nuclei is consistent with the small deviations of the observed g tensors from the spin only (g_e) value.[11,12] Our calculated values (in D_{3h}) for the total hyperfine tensors (A_{ii}) show a fairly good agreement with those reported experimentally (within 12%–15%). Some rhombic character in A_{ii} appears in our calculation, and the origin of this effect probably arises from contributions from the $j = \frac{3}{2}$ or $j = \frac{5}{2}$ state to the HOMO. This suggests some degree of magnetic inequivalency between the equatorial Ag nuclei, since the hyperfine tensors reflect the symmetry of the electronic distribution at this center (see Fig. 1) which is not necessarily the symmetry of the cluster.[14] Our calculated results of the DSW calculations on the open C_{2v} structure of Ag_5 are also presented in Table III. Our results also predict the larger hfi for the two equatorial centers (as assigned in the ESR study[11,12]); but the calculated hfi differ considerably from the experimental values.

In addition, in Table III, we also compare our calculated values (for D_{3h}) with the experimentally determined values

TABLE III. Hyperfine coupling constants[a] for $^{107}Ag_5$.

	Ax			Eq		
	DSW(D_{3h})	DSW(C_{2v})	Expt	DSW(D_{3h})	DSW(C_{2v})	Expt
Fermi term	1.1[b]	1.7	···	− 186.6	− 361.9	210.7[c]
Spin-dipolar term	0.8[d]	1.4	···	1.5	0.2	0.8[c]
Orbital term[d]						
$l_{xx} = l_{yy}$	− 3.6	− 1.7	···	2.8	− 19.6	···
l_{zz}	7.1	− 4.6	···	5.7	− 0.7	···
Total A_{ii}[e]						
A_{xx}	− 3.3	− 1.4	5.5[f]	− 188.1	− 381.7	211.6[f]
A_{yy}	− 3.3	− 1.4		182.6	− 381.7	
A_{zz}	9.8	0.9	11.0[f]	− 177.9	− 362.1	209.1[f]

[a] All values in G.
[b] Diagonal contributions from the $5s_{1/2}$ waves, see the text.
[c] Experimental estimates (Refs. 11 and 12).
[d] See the text for the method of calculation.
[e] DSW values for the remaining Eq are: $A_{xx} = 0.2$ and $A_{zz} = -10.1$.
[f] Expt values (Refs. 11 and 12) assigned to a distorted D_{3h} geometry in $^2B_2$ (C_{2v}) ground state, see the text. Sign is not determined experimentally.

for the superhyperfine interactions that arise from the axial centers of Ag_5 and we observe a very good agreement for the total A_{ii}. It is interesting to note that a small Fermi term (1.1 G) arises due to spin-orbit mixings in the HOMO, which is a relativistic effect, since the Fermi term vanishes by symmetry in the NR limit. Furthermore, it should be noted that in the ESR study,[11] a small percentage of negative unpaired 5*s* spin population has been assigned to the axial Ag nuclei, which may account for the origin of the small calculated Fermi term arising from a spin transfer to the axial Ag nuclei. It can be seen from Table III, that the orbital contributions for the axial Ag centers are of the same order of magnitude as that of A_{ii}, and that $A_{\rm dip}$ has a smaller contribution to the axial hyperfine tensors. It is pointed out, that our calculated values (for D_{3h}) are within 10% to 15% of the experimental values. This level of agreement has been obtained previously for heavy diatomic radicals,[16] transition metals,[23] lanthanide,[22] and actinide[24] complexes, as well as in silver and gold clusters.[25] In conclusion, from our calculated results (for the D_{3h} and C_{2v} geometries) and due to the twofold spin degeneracy (Kramers degeneracy) of the ground state of Ag_5 cluster, we are led to conclude that the Jahn–Teller[35] distortion of D_{3h} geometry to C_{2v} is highly improbable. Furthermore, the Cu_5 and Ag_5 clusters are not expected to be similar, since relativistic effects (notably spin-orbit interaction) in Ag_5 are expected to be more pronounced than in Cu_5.

2. Ag_5^{2+} and Ag_5^{4+}

The hyperfine tensor (A_{ii}) components of the trigonal bipyramidal Ag_5^{2+} and Ag_5^{4+} clusters have been predicted by OMM[14] through nonrelativistic scattered-wave calculations, in which the spin-orbit and the nuclear hyperfine interactions were treated as perturbations to the Schrödinger Hamiltonian.[14] In this procedure originally developed by Keijzer and de Boer,[37] the spin Hamiltonian parameters are calculated in terms of the coefficients of nonrelativistic molecular orbital wave functions. Basically, a second order perturbation approach was used to calculate the hyperfine coupling of the electronic spin S with the spin I of the nuclei. In this way, the first order contributions to A_{ii} are given by evaluating the matrix elements of the spin-dipolar operator; whereas the spin-orbit and orbital interactions are calculated as the second order contributions to the hyperfine coupling tensor. The energies of the states are then calculated by summing (one-electron MO energies) over all possible excited states.[14,37]

Although this theory has been shown to be successful in calculating hfi in some copper–carbamate complexes,[37] it suffers from the following disadvantages in quantitative applications: (a) To estimate reliably the excitation energies (in systems containing heavy atoms) by means of nonrelativistic calculations would be inadequate, since the relativistic shift of the energy levels could be significant, and in addition, in some cases the continuum contribution is important.[38] (b) Additional terms must be added to obtain a gauge invariant MO theory[37] and in practical applications some approximations are generally made.[14] (c) The question of convergence of the perturbation series is rarely addressed, and it has been shown that third order effects can be important in the magnetic resonance parameters of many Co(II) complexes.[39] (d) It has been noted[22,40] that the use of molecular orbital coefficients in calculating g and A tensors has serious problems.

A more direct method of calculating magnetic resonance parameters uses the DSW four-component wave function to account for the approximate g or hyperfine tensors.[16,19,22–25] Using a Dirac calculation as our zeroth order wave function (which includes spin-orbit effects), we can revert to first order perturbation theory for the description of hyperfine effects, in which the only perturbation is the hyperfine energy.[16,19] Since the α matrices are off-diagonal [see Eq. (2)], the evaluation of the matrix elements involves products of the "large" and "small" components of the wave function.[16,19] Thus, the magnetic interactions involve contributions from both the large and the small components. Furthermore, the expression in Eq. (4) includes the contact, dipolar, and orbital terms, and there is no need to use different operators to represent these terms, as in nonrelativistic theories.[16,19] However, the total hyperfine tensor can be approximately partitioned into Fermi contact, spin dipolar, and orbital terms, as was done above for Ag_5. The relation between the nonrelativistic and relativistic perturbation Hamiltonian has been discussed earlier.[41] Here, we also report the calculated hfi values of the nonrelativistic limit (NR) allowing us to ascertain the relativistic effects in magnetic interactions. As $c \to \infty$, the small components approach zero at the same rate as the bohr magneton (β_e). Hence, the elements of the hyperfine tensors divided by β_e approach a definite NR limit. We have verified numerically that the hyperfine tensors derived from a DSW calculation with $c = 10^{15}$ a.u. agree exactly with the results of a nonrelativistic scattered-wave calculation in which the usual Fermi contact and spin-dipolar operators are employed.[16,19] Hence, the present study offers a good opportunity to compare our fully relativistic (DSW) and the NR limit hfi calculations with those reported by OMM,[14] and as we describe below, significant differences are observed between the calculated hfi using the two approaches.

In Table IV we present the spin populations of Ag_5^{2+} as calculated by the DSW and its NR limit ($c \to \infty$). The charge breakdown is given in terms of the nonrelativistic functions multiplied by the spin functions (Pauli), and in terms of the atomic spinors (DSW). It can be seen that the major contribution to the HOMO ($9e_2$ or $3a_2''$) arises from the axial Ag nuclei and is mainly of 5*s* ($\sim$65%) character. This result should be compared with those of OMM (see Table VI, in Ref. 14) which assigned a contribution of $\sim$74% (5*s*). It should be remarked that our spin populations were calculated according to the algorithm of Case and Karplus,[32] in which the intersphere and outersphere charges has been partitioned among the atoms using weights proportional to the surface charge distribution on each atom. This procedure usually gives very good agreement with the experimental estimates of spin populations.[16,19,22–24] The procedure utilized by OMM is based on a simple reallocation of the intersphere charge that is proportional to the existing charge within each sphere.[14] Since the present and the OMM

TABLE IV. Spin populations of Ag_5^{2+}.

	Dirac			Pauli			
	l	j	Population	l	m	Spin	Population
(A) Relativistic ($9e_2$)							
	s	$\frac{1}{2}$	0.664	s	0	α	0.664
	p	$\frac{1}{2}$	0.002	p	0	α	0.008
Ax	p	$\frac{3}{2}$	0.006	p	1	β	a
	d	$\frac{3}{2}$	a	d	0	α	a
	d	$\frac{5}{2}$	a	d	1	β	a
				d	-2	β	a
	s	$\frac{1}{2}$	0.003	s	0	β	0.003
	p	$\frac{1}{2}$	0.092	p	0	α	0.240
Eq	p	$\frac{3}{2}$	0.148	p	1	β	a
	d	$\frac{3}{2}$	0.030	d	-1	α	0.040
	d	$\frac{5}{2}$	0.054	d	1	α	0.044
(B) Nonrelativistic ($3a_2''$)							
	s	$\frac{1}{2}$	0.648	s	0	α	0.648
	p	$\frac{1}{2}$	0.004	p	0	α	0.012
Ax	p	$\frac{3}{2}$	0.008	d	0	α	a
	d	$\frac{3}{2}$	a				
	d	$\frac{5}{2}$	a				
	s	$\frac{1}{2}$	b	s	0	α	b
	p	$\frac{1}{2}$	0.090	p	0	α	0.027
Eq	p	$\frac{3}{2}$	0.180	d	-1	α	0.035
	d	$\frac{3}{2}$	0.028	d	1	α	0.035
	d	$\frac{5}{2}$	0.042				

[a] Contributions are less than 0.001.
[b] Values are zero because of symmetry.

calculations employ basically the same geometrical and calculational parameters, the differences that arise in the calculated values for the spin populations are attributed to the different procedures used by both approaches.

It can be seen from Table IV, that in the equatorial centers there are small 5*s* contributions (0.3%) which arise from spin-orbit mixings into the HOMO; this contribution is not present in the NR limit, which implies that a small Fermi term will arise in the hfi DSW calculation, which vanishes by symmetry in the NR limit. As indicated in Table IV, the nonrelativistic HOMO ($3a_2''$) shows pure spin (α) states, while the relativistic HOMO ($9e_2$) shows contributions of mixed spin; however, the minority spin (β) contributions are very small (0.4%), implying a small orbital term contribution to the hyperfine tensors.

The hyperfine coupling constants of Ag_5^{2+} are given in Table VI, as calculated by OMM,[14] the DSW method and its NR limit. If one compares the Fermi term calculated by all of these approaches, one can see that the DSW and the OMM results disagree by $\sim 40\%$, while the OMM and the NR limit calculated values disagree by $\sim 20\%$. Furthermore, the OMM values are the smallest of all, besides the fact that their calculated 5*s* spin populations are larger (by $\sim 10\%$) than that calculated in the present study. This result further suggests that the use of nonrelativistic molecular orbital coefficient is not appropriate for calculating magnetic interactions. If we compare the Fermi term as calculated by the NR limit and the DSW method, we observe that the larger DSW values imply a greater 5*s* spin density (in the axial Ag nuclei), as expected due to relativistic effects. The difference between these two values is an evidence that the matrix elements of $(\alpha \times r)$ are not proportional to the net charge inside the spheres (since the NR and the DSW populations are about the same, see Table IV). Since the Fermi contact term is the major contributor to the hyperfine tensors, these are mostly *isotropic* and the three methods of calculation agree at this point. In Table VI we also present the spin-dipolar and orbital terms, which represent small contributions to the total hyperfine tensors. By examining the calculated hfi of the equatorial Ag nuclei, we observe a small Fermi term which arises due to spin transfer, and this term vanishes by symmetry in the NR calculations. Again, there are numerical differences between the OMM results and those obtained in the present study. The hyperfine tensors for the equatorial Ag nuclei are mostly *anisotropic* and the DSW results show that substantial spin dipolar and orbital terms arise due to 4*d* contributions to the HOMO. The OMM results (for the total hyperfine tensors) are smaller than the NR limit and the DSW calculations by a factor of 2, and this is consistent with their neglect of the 4*d* contributions. It can be concluded that the hfi calculations for Ag_5^{2+} clearly reveal that the second order perturbational procedure used by OMM[14] seriously underestimates the magnetic hyperfine interactions, since it gives smaller values than the

NR limit and the DSW calculation. Furthermore, the use of four-component wave functions should be more appropriate since the small components also contribute to the calculation of the hyperfine coupling constants. The importance of the small components in hfi has been recently analyzed through relativistic and NR calculations in gold atom. In the NR calculation the magnetic interaction is dominated entirely by the Fermi contact term, whereas in the relativistic calculation the Fermi term arises from the large components of the wave function; in addition, substantial spin-dipolar and orbital contributions arise from the small components.[42] In the Ag_5^{2+} cluster, the relativistic and the NR spin-dipolar contributions are virtually the same, indicating thereby that the large components (DSW) dominate this term. However, as the spin-orbit mixings to the HOMO are small (0.4%), the orbital terms probably arise due to the small components of the molecular wave function; these orbital terms in the case of the equatorial Ag nuclei are substantial and negative compared to the total A_{ii} values.

In Table V the calculated spin populations of Ag_5^{4+} are shown. It can be seen that the NR limit populations are pure β spin states, while the DSW calculation shows states of mixed spin. The spin α contamination to the HOMO ($9e_1$) is 1.5% and is larger than in Ag_5 and Ag_5^{2+}. In other words, there is an excess of 0.97 electrons of spin β over the spin α, while in the NR limit this excess is 1.0. Most of the spin α contamination arises from the 4*d* contributions to axial Ag nuclei. Hence, it is expected that the orbital contributions to the hyperfine tensors will be larger in the axial Ag nuclei. It is interesting to note that the population analysis of OMM for this MO ($4a_1'$, see Table VI in Ref. 14) assigns only 6.2% 4*d* participation, whereas our NR limit results assign 14% 4*d* contributions. These should be compared with the DSW populations which assign 26% 4*d* character into the HOMO. Obviously, this is a relativistic effect which is due to the destabilization of the MO's that consist largely of 4*d* AO's and the stabilization of MO's that contain significant 5*s* character. The HOMO level of Ag_5^{4+} is strongly bonding and upon inclusion of relativity a significant *s*–*d* hybridization occurs; this is illustrated in Figs. 4 and 6. As shown in Table V the NR limit result shows significant contributions from the 5*s* atomic orbitals to the axial ($\sim$19%) and equatorial ($\sim$50%) Ag nuclei. These populations should be compared with those calculated by OMM, which are 23% and 59%, respectively.

The hyperfine coupling constants for Ag_5^{4+} as calculated by OMM,[14] the NR limit and the DSW method are given in Table VI. It should be remarked that in their calculations

TABLE V. Spin populations of Ag_5^{4+}.

	Dirac			Pauli			
	l	*j*	Population	*l*	*m*	Spin	Population
(A) Relativistic ($9e_1$)							
	s	$\frac{1}{2}$	0.186	*s*	0	β	0.186
	p	$\frac{1}{2}$	0.018	*p*	0	β	0.052
Ax	*p*	$\frac{3}{2}$	0.034	*d*	−1	α	0.012
	d	$\frac{3}{2}$	0.033	*d*	0	β	0.174
	d	$\frac{5}{2}$	0.153				
	s	$\frac{1}{2}$	0.441	*s*	0	β	0.441
	p	$\frac{1}{2}$	0.021	*p*	0	α	a
Eq	*p*	$\frac{3}{2}$	0.048	*p*	1	β	0.034
	d	$\frac{3}{2}$	0.009	*p*	−1	β	0.034
	d	$\frac{5}{2}$	0.057	*d*	−1	α	a
				d	0	β	a
				d	1	α	0.003
				d	2	β	0.020
				d	−2	β	0.043
(B) Nonrelativistic ($4a_1'$)							
	s	$\frac{1}{2}$	0.195	*s*	0	β	0.196
	p	$\frac{1}{2}$	0.022	*p*	0	β	0.066
Ax	*p*	$\frac{3}{2}$	0.044	*d*	0	β	0.095
	d	$\frac{3}{2}$	0.038				
	d	$\frac{5}{2}$	0.057				
	s	$\frac{1}{2}$	0.500	*s*	0	β	0.500
	p	$\frac{1}{2}$	0.033	*p*	1	β	0.050
Eq	*p*	$\frac{3}{2}$	0.066	*p*	−1	β	0.049
	d	$\frac{3}{2}$	0.018	*d*	0	β	0.002
	d	$\frac{5}{2}$	0.027	*d*	2	β	0.022
				d	−2	β	0.022

[a] Contributions are less than 0.001.

TABLE VI. Hyperfine coupling constants[a,b] for Ag_5^{2+} and Ag_5^{4+}.

	Ag_5^{2+}		Ag_5^{4+}	
	Ax	Eq	Ax	Eq
Fermi term				
OMM	227.8	c	70.7	121.3
NR	284.6	c	− 86.9	− 165.5
DSW	383.5	− 0.9	− 103.7	− 180.6
Spin dipolar term				
NR	− 0.4	− 6.2	− 4.6	2.1
DSW	− 0.4	− 6.3	− 5.9	1.9
Orbital term				
DSW for $l_{xx} = l_{yy}$	− 0.5	2.4	− 11.9	− 0.6
l_{zz}	1.0	− 6.8	6.0	− 3.8
Total A_{xx}				
OMM	227.5	− 0.7	d	d
NR	284.4	− 2.3	− 84.6	− 168.6
DSW	383.4	− 5.3	− 109.7	− 182.5
Total A_{yy}				
OMM	227.5	− 0.7	d	d
NR	284.4	− 3.9	− 84.6	− 164.4
DSW	383.4	− 4.3	− 109.7	− 183.8
Total A_{zz}				
OMM	228.1	3.7	d	d
NR	285.1	6.1	− 91.4	− 163.5
DSW	383.7	6.7	− 109.5	− 182.1

[a] All values calculated for ^{109}Ag ($g_N = -0.261$) in G.

[b] Abbreviations: OMM, nonrelativistic scattered wave and second order perturbation approach (see Ref. 14); NR, nonrelativistic limit; DSW, Dirac scattered wave and first order perturbation.

[c] Values vanish by symmetry.

[d] It was assumed that hfi splitting arises only from the Fermi term (Ref. 14).

OMM assumed that the hyperfine splittings arise only from the isotropic Fermi contact term; in other words, they neglected the 5*p* and 4*d* contributions to the HOMO.[14] Even then the results of OMM show larger 5*s* contributions than the present study, and their calculated Fermi term is smaller than that calculated here by the DSW method and its NR limit. Thus, it is clearly evident that the use of molecular orbital coefficients to calculate the spin Hamiltonian parameters is inadequate, at least for the cases studied here. Our results indicate that the hyperfine tensors (for Ag axial and Ag equatorial, respectively), are mostly *isotropic*, however, there are small but nonnegligible contributions from the spin-dipolar and orbital terms. In fact, the orbital terms for Ag (axial) represent about 11% of the total A_{ii} values, and the spin-dipolar contributions represent only a 5% to the A_{ii}'s.

It can be concluded that the relativistic effects on hyperfine interactions for the Ag_5^{2+} and the Ag_5^{4+} clusters are manifested mainly in the Fermi contact term and to a lesser degree in the small orbital contributions to the hyperfine tensors. Furthermore, it is clearly demonstrated that the second order nonrelativistic perturbational procedure, together with the use of molecular orbital coefficients underestimate the magnetic hyperfine interactions, since these calculated values are always smaller than the NR limit (by ~20%) and the fully relativistic (by ~40%) results. Even for the high symmetry silver clusters studied here, the large differences between the four-component and the one-component results (based on larger calculated spin density) cast some doubt on the assumption of the traditional theory, viz., the neglect of the small components of the wave function and of the difference between the $j = l + \frac{1}{2}$ and $j = l - \frac{1}{2}$ sublevels.

C. Transition state calculations

The use of the Slater's transition state (TS) method[21] is a convenient approach within the local density theory to estimate relaxation corrections (upon electron excitation) to excitation energies. In principle, the highest accuracy is obtained by doing separate transition state calculations (until SCF convergence is reached) for every transition of interest. In particular, it is known that relaxation corrections are generally independent of the particular molecular orbitals involved.[22] The predicted excitation energies for the lowest allowed electronic transitions from the ground state HOMO to the unoccupied orbitals for each cluster are collected in Table VII. We also show the energy difference in the relativistic ground state (DSW-GS) eigenvalues, the difference in nonrelativistic state (OMM-GS) eigenvalues, as calculated by OMM,[14] the relaxation corrections (Δ_1), and finally, the differences between the relativistic and the nonrelativistic

TABLE VII. Excitation energies[a] for Ag_5^{q+} clusters.

Cluster	Transition	DSW-TS[b]	DSW-GS[c]	Δ_1[d]	OMM-GS[e]	Δ_2[f]
	$10e_2 \rightarrow 10e_1$	13454	12597	857	14513	−1986
	$10e_2 \rightarrow 11e_1$	21695	21112	583	20964	148
Ag_5	$10e_2 \rightarrow 12e_1$	23900	23284	626	21598	1686
	$10e_2 \rightarrow 11e_3$	24557	23803	754	21598	2205
	$9e_2 \rightarrow 10e_1$	20486	20541	−55	20746	−205
Ag_5^{2+}	$9e_2 \rightarrow 11e_1$	32826	31965	861	29411	2554
	$9e_2 \rightarrow 11e_3$	35488	34938	550	29940	4998
	$9e_1 \rightarrow 9e_2$	25992	25468	524		
	$9e_1 \rightarrow 10e_2$	33126	32500	626		
Ag_5^{3+}	$9e_1 \rightarrow 10e_3$	33664	33089	575		
	$9e_1 \rightarrow 11e_3$	63817	63390	427		
	$9e_1 \rightarrow 9e_2$	27625	27240	385	25252	1988
Ag_5^{4+}	$9e_1 \rightarrow 10e_2$	33892	34300	−404	30211	4089
	$9e_1 \rightarrow 10e_3$	35296	34812	484	30211	4601
	$9e_1 \rightarrow 11e_3$	67767	67428	339		

[a] All values in cm^{-1}.
[b] TS = transition state calculation.
[c] Difference in relativistic ground state (GS) eigenvalues.
[d] Relaxation corrections.
[e] Difference in nonrelativistic ground state eigenvalues (Ref. 14).
[f] Difference between GS (relativistic and nonrelativistic) eigenvalues.

ground state eigenvalues (Δ_2), in order to calculate the relativistic corrections to the excitation energies estimated by OMM.[14] It can be seen from Table VII, that as charge is depleted from the HOMO's the HOMO–LUMO transition occurs at lower wavelength. Thus, Ag_5 absorbs at the IR region, indicating a colorless reflection which is characteristic of the bulk metal. OMM predict this transition to occur at the red region, indicating a green reflection. While, Ag_5^{2+} is predicted to absorb at the blue region, Ag_5^{q+} ($q = 3$ and 4) is expected to absorb at the violet region of the electromagnetic spectrum. It is interesting to note, that as the cluster size increases the HOMO–LUMO transition occurs at larger wavelength, for instance, Ag_3^{2+} absorbs at 415 nm[25], whereas Ag_5^{2+} absorbs at 743 nm. The same trend has been observed in the UV and visible absorption spectral studies of small silver aggregates.[7–9] The relaxation corrections (Δ_1) are of the order of 300–800 cm^{-1}, as indicated in Table VII, and their negative signs indicate that the energy gap obtained in the TS calculation is smaller than in the GS calculation. By comparing the eigenvalue differences (Δ_2) between the ground state DSW and the OMM approaches, one can appreciate the magnitude of the relativistic effects in estimated excitation energies, and these effects are usually significant. Moreover, relativistic effects of the similar order of magnitude would be expected in the calculation of excitation energies for other electronic transitions reported by OMM,[14] and since these excitations are required [see Eq. (11) of Ref. 14] in the second order perturbation treatment[14,37] for the calculation of molecular hyperfine coupling constants, one would expect large differences between the hfi values calculated by the DSW and OMM methods.

The predicted first ionization potential (I.P.) as calculated by the DSW-TS and the NR-SW-TS (OMM)[14] approaches are presented in Table VIII. It can be seen that relativistic effects influence the first I.P., and that these effects become larger as charge is progressively depleted from the HOMO's. In addition, it is interesting to note that the first I.P. decreases upon increasing the cluster size, e.g., the calculated first I.P. for Ag_3^{2+} is 19.4 eV,[25] whereas the I.P. for Ag_5^{2+} is only 16.4 eV.

IV. CONCLUSIONS

Our results indicate that the relativistic effects cannot be neglected in these pentaatomic silver clusters. In particular, the nature of bonding in these clusters differs from the nonrelativistic description; since due to relativistic effects the cluster bonding is dominated by $5s_{1/2}$–$4d_{5/2}$ hybrid molecular orbitals. It is also pointed out from double group symmetry considerations that Jahn–Teller distortion is very unlikely to be operative in Ag_5. Our results of the relativistic hfi calculations indicate that the relativistic effects are manifested mainly in the Fermi contact term, and in addition, give rise to small orbital contributions to the molecular hyperfine tensors. Moreover, it is demonstrated that the second order nonrelativistic perturbational procedure, using molecular orbital coefficients underestimates the magnetic hyperfine interactions in Ag_5^{2+} and Ag_5^{4+}. Finally, the first ionization

TABLE VIII. Predicted first ionization potentials (I.P.).

	DSW-TS		OMM-TS[a]	
Cluster	HOMO	First I.P. (eV)	HOMO	First I.P. (eV)
Ag_5	$(10e_2)^1$	6.8	$(6e')^1$	6.5
Ag_5^{2+}	$(9e_2)^1$	16.4	$(3a_2'')^1$	15.6
Ag_5^{3+}	$(9e_1)^2$	24.7	$(4a_1')^2$	23.2
Ag_5^{4+}	$(9e_1)^1$	29.9	$(4a_1')^1$	27.9

[a] Reference 14.

potentials of these clusters are predicted to be larger due to relativistic effects which increase as charge is depleted from the HOMO's .

We believe that the DSW method can be a good qualitative guide in analyzing photoelectron, optical and ESR spectra of clusters containing heavy atoms, and further work is in progress on larger clusters containing heavier atoms.

ACKNOWLEDGMENTS

We are grateful to Professor David Case for valuable suggestions and discussions. We thank the Natural Sciences and Engineering Research Council (NSERC) of Canada for a Grant No. A3598 as well as for a grant for the use of the CRAY-1 computer at Dorval, Montreal.

[1]Faraday Symp. Chem. Soc. **14**, 3–350 (1980).
[2]Proceedings of a symposium on Small Particles and Inorganic Cluster, Surf. Sci. **156** (1985), parts I and II.
[3]R. van Hardeveld and F. Hartog, Adv. Catal. **22**, 75 (1972); P. Fayet, F. Granzer, G. Hegenbart, E. Moisar, B. Pischel, and L. Woste, Phys. Rev. Lett. **55**, 3002 (1985).
[4]G. A. Ozin, Faraday Symp. Chem. Soc. **14**, 7 (1980).
[5]J. A. Howard, K. F. Preston, and B. Mile, J. Am. Chem. Soc. **103**, 6226 (1981).
[6]K. Kernisant, G. A. Thompson, and D. M. Lindsay, J. Chem. Phys. **82**, 4739 (1985).
[7]W. Schulze, H. U. Becker, and H. Abe, Chem. Phys. **35**, 177 (1978).
[8]G. A. Ozin and H. Huber, Inorg. Chem. **17**, 155 (1978).
[9]S. A. Mitchell and G. A. Ozin, J. Phys. Chem. **88**, 1425 (1984).
[10]D. Hermerschmidt and R. Haul, Ber. Bunsenges. Phys. Chem. **84**, 902 (1980); P. J. Grobet and R. A. Schoonheydt, Surf. Sci. **156**, 893 (1985).
[11]J. A. Howard, R. Sutcliffe, and B. Mile, J. Phys. Chem. **87**, 2268 (1983).
[12]J. A. Howard, R. Sutcliffe, and B. Mile, Surf. Sci. **156**, 214 (1985).
[13]C. Bachman, J. Demuynck, and A. Veillard, Faraday Symp. Chem. Soc. **14**, 170 (1980).
[14]G. A. Ozin, S. M. Mattar, and D. F. McInstosh, J. Am. Chem. Soc. **106**, 7765 (1984).
[15](a) K. H. Johnson, Adv. Quantum Chem. **7**, 143 (1973); (b) C. Y. Yang and S. Rabii, Phys. Rev. A **12**, 362 (1975).
[16]R. Arratia-Perez and D. A. Case, J. Chem. Phys. **79**, 4939 (1983).
[17]C. Y. Yang, in *Relativistic Effects in Atoms, Molecules and Solids*, edited by G. L. Malli (Plenum, New York, 1983), p. 335.
[18]D. A. Case, Annu. Rev. Phys. Chem. **33**, 151 (1982).
[19]C. Y. Yang and D. A. Case, in *Local Density Approximations in Quantum Chemistry and Solid State Physsics*, edited by J. Dahl and J. P. Avery (Plenum, New York, 1984), p. 643.
[20]M. E. Rose, *Relativistic Electron Theory* (Wiley, New York, 1961).
[21]J. C. Slater, *The Self-Consistent Field for Molecules and Solids* (McGraw–Hill, New York, 1974).
[22]D. A. Case and J. P. Lopez, J. Chem. Phys. **80**, 3270 (1984).
[23]J. P. Lopez and D. A. Case, J. Chem. Phys. **81**, 4554 (1984).
[24]D. A. Case, J. Chem. Phys. **83**, 5792 (1985).
[25]R. Arratia-Perez and G. L. Malli, J. Chem. Phys. **84**, 5891 (1986).
[26]C. Y. Yang, J. Chem. Phys. **68**, 2626 (1978).
[27]G. F. Koster, J. O. Dimmock, R. G. Wheeler, and H. Statz, *Properties of the 32 point groups* (MIT, Cambridge, 1963).
[28]The conversion of the DSW code to the CRAY-1 computer was done by R. Arratia-Perez in 1985.
[29]G. Apai, S. T. Lee, and M. G. Mason, Solid Stat. Commun. **37**, 213 (1981).
[30]A. D. McLachlan, J. Liesegan, R. C. G. Leckey, and J. G. Jenkin, Phys. Rev. B **11**, 2877 (1975).
[31]*Relativistic Effects in Atoms, Molecules and Solids*, edited by G. L. Malli (Plenum, New York, 1983).
[32]D. A. Case and M. Karplus, Chem. Phys. Lett. **39**, 33 (1976).
[33]G. H. Jeung, M. Pelissier, and J. C. Berthelat, Chem. Phys. Lett. **97**, 369 (1983); S. W. Wang, J. Chem. Phys. **82**, 4633 (1985).
[34]J. A. Howard, R. Sutcliffe, J. S. Tse, and B. Mile, Chem. Phys. Lett. **94**, 561 (1983).
[35]H. A. Jahn, Proc. R. Soc. London Ser. A **164**, 117 (1938); H. A. Jahn and E. Teller, *ibid.* **161**, 220 (1937).
[36]W. Weltner, Jr. and R. van Zee, Annu. Rev. Phys. Chem. **35**, 291 (1984).
[37]C. P. Keijzer and E. de Boer, J. Chem. Phys. **57**, 1277 (1972).
[38]J. Andriessen, R. Chatterjee, and D. van Ormondt, J. Phys. C **7**, L339 (1974).
[39]B. R. McGarvey, Can. J . Chem. **53**, 2498 (1975).
[40]S. F. Sontum and D. A. Case, J. Phys. Chem. **86**, 1596 (1982); D. A. Case and M. Karplus, J. Am. Chem. Soc. **99**, 6182 (1977).
[41]I. Lindgren and A. Rosen, Case Stud. At. Phys. **4**, 97 (1974).
[42]N. C. Pyper (personal communication).